ELSEVIER

Physica B 234–236 (1997) 821–829

PHYSICA B

Spin excitations and phonons in $YBa_2Cu_3O_{6+x}$: A status report

B. Keimer[a,b,*], I.A. Aksay[c], J. Bossy[d], P. Bourges[e], H.F. Fong[a], D.L. Milius[c], L.P. Regnault[f], D. Reznik[e,1], C. Vettier[g]

[a] *Department of Physics, Princeton University, Princeton, NJ 08544, USA*
[b] *Department of Physics, Brookhaven National Laboratory, Upton, NY 11973, USA*
[c] *Department of Chemical Engineering, Princeton University, Princeton, NJ 08544, USA*
[d] *Institut Laue-Langevin, 38042 Grenoble, Cedex, France*
[e] *Laboratoire Léon Brillouin, CEA-CNRS, CEA-Saclay, 91191 Gif-sur-Yvette, France*
[f] *Département de Recherche Fondamentale sur la Matière Condensée, Service de Physique Statistique, Magnétisme et Supraconductivité, Groupe Magnétisme et Diffraction Neutronique, CEA-Grenoble, 38054 Grenoble, Cedex 9, France*
[g] *European Synchrotron Research Facility, Boîte Postale No. 220, 38043 Grenoble, Cedex, France*

Abstract

A review is made of recent developments in inelastic neutron scattering experiments on spin excitations and phonons in the high-temperature superconductor $YBa_2Cu_3O_{6+x}$ and its antiferromagnetic precursor $YBa_2Cu_3O_{6.2}$. These experiments include the detection of high-energy "optical" spin waves and the determination of the full spin Hamiltonian in $YBa_2Cu_3O_{6.2}$, detailed investigations of the 40 meV magnetic resonance peak in the superconducting state of $YBa_2Cu_3O_7$ and its precursors in underdoped $YBa_2Cu_3O_{6+x}$, and experiments on the effect of superconductivity on phonon lifetimes in $YBa_2Cu_3O_7$.

Keywords: Spin excitations; Phonons; $YBa_2Cu_3O_{6+x}$

1. Introduction

Neutron scattering is the only probe capable of providing maps of the magnetic and lattice vibrational excitation spectra of materials over the entire Brillouin zone. In complex materials such as the high-T_c cuprates one cannot hope to arrive at a quantitative theory without experimental information about these excitations. More specifically, strong electron–electron interactions are now generally recognized as central to the physics of these materials. Energy and momentum-dependent enhancements of the dynamic spin susceptibility $\chi''(\boldsymbol{q},\omega)$ are a direct consequence of these interactions and provide incisive microscopic constraints on theories of superconductivity. Since large, high-quality single crystals are available, the $YBa_2Cu_3O_{6+x}$ family offers a unique opportunity to explore the evolution of the spin excitation spectrum by neutron scattering as the material evolves from an antiferromagnetic insulator to a high-temperature superconductor with increasing x. Much progress has been made during the last decade [1–3], but this field is still in a stage of rapid development, mostly due to the intrinsic difficulty of the experiments. This paper summarizes recent progress made by our groups which was made possible by the growth of very large single crystals at Princeton University.

* Corresponding author.
[1] Present Address: Department of Physics, UCSD, La Jolla, CA 92093, USA.

PII S0921-4526(96)01111-8

We are ultimately interested in the pairing mechanism in these materials and have thus focused on the temperature evolution of the magnetic excitation spectrum through the superconducting transition. Early indications of effects of superconductivity on the spin excitation spectrum of $YBa_2Cu_3O_7$ [4, 5] have recently been followed by detailed, quantitative studies [6, 7]. These experiments have revealed a strikingly sharp magnetic resonance mode in the superconducting state which disappears in the normal state. This novel collective mode has stimulated much theoretical work, and its interpretation is still controversial. In an effort to discriminate between different theoretical models we recently traced the evolution of the resonance with doping into the deeply underdoped regime [8, 9].

Further, it has now become possible to extend earlier investigations of low-energy spin excitations [1–3] to energies high enough to excite antiphase motion of spins in directly adjacent layers (the bilayers) [10]. Detection of such "optical" spin waves in the antiferromagnetic phase allows one to deduce the exchange coupling between the bilayers, an important parameter in the Hamiltonian of these materials. Very recently, we have also observed such antiphase spin excitations in the metallic regime [11].

Finally, while the intrinsic lifetimes of phonons have been studied extensively at $\boldsymbol{q} = 0$ by Raman scattering, insufficient energy resolution has until recently prevented an extension of these studies to nonzero $\boldsymbol{q}$. Such experiments are important because valuable information about the electron–phonon coupling and the nature of the pairing state can be extracted from the renormalization of phonon lifetimes below the superconducting transition temperature. We give a brief review of our recent work on this problem [12].

2. Optical spin waves in antiferromagnetic $YBa_2Cu_3O_{6.2}$

For oxygen concentrations $x \lesssim 0.4$, $YBa_2Cu_3O_{6+x}$ is an antiferromagnetically long-range ordered insulator with a spin structure shown in Fig. 1(a). As there are two spins per chemical unit cell, the spin wave spectrum consists of an optical and an acoustic branch. Pictorial representations of these two types of spin excitation are given in Fig. 1(b). For a long wavelength optical spin wave, spins located in directly adjacent layers precess in antiphase (Fig. 1(b)). While acoustic spin waves have only a small gap due to exchange anisotropies and interbilayer exchange, the optical magnon branch has a much larger gap because the exchange interactions between nearest-neighbor spins within the same bilayer are very strong. Detailed calculations [1] reveal that the optical magnon gap is given by

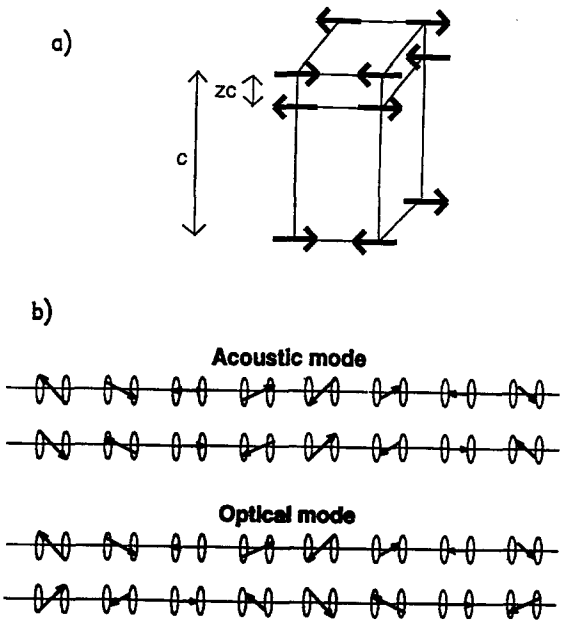

Fig. 1. (a) Spin structure of antiferromagnetic $YBa_2Cu_3O_{6+x}$ ($x \lesssim 0.4$). (b) Sketches of acoustic and optical spin waves.

$$E_{\mathrm{opt}} \sim 2\sqrt{J_{\perp}J_{\parallel}}, \tag{1}$$

where $J_{\parallel} \sim 120$ meV is the nearest-neighbor superexchange in the CuO_2 plane which is known from measurements of the slope of the dispersion of low-energy acoustic spin waves (spin wave velocity) and from two-magnon Raman scattering. The value of $J_{\perp}$, the superexchange coupling between nearest neighbors in the c-axis direction perpendicular to the CuO_2 planes, had been unknown until recently. (For the sake of simplicity, small corrections to Eq. (1) due to spin–orbit coupling and superexchange coupling between different bilayers as well as somewhat larger corrections due to quantum renormalization of the spin wave velocity are ignored in the present discussion.)

The cross sections for neutron scattering from acoustic and optical spin waves contain different dynamical structure factors which can be thought of as the Fourier transforms of the real space pictures of Fig. 1(b), quite analogous to the more familiar static structure factors in X-ray or neutron diffraction. These are proportional to $\sin^2(\pi Q_\perp zc)$ for acoustic magnons and $\cos^2(\pi Q_\perp zc)$ for optical magnons, where $Q_\perp$ is the momentum transfer perpendicular to the CuO_2 sheets. We [10] have recently carried out high-energy magnetic scattering experiments on $YBa_2Cu_3O_{6.2}$, and have exploited these different structure factors to separate optical from acoustic spin waves. We found that the optical spin wave gap is $E_{opt} \sim 70$ meV, which translates into $J_\perp \sim 10$ meV according to Eq. (1). This value is in good agreement with recent predictions of band theory [13]. A subsequent report by Hayden et al. [14] appears consistent with this result.

As the superexchange coupling is generally proportional to the square of the overlap of the electronic wave functions, we have

$$\frac{t_\perp}{t_\parallel} = \sqrt{\frac{J_\perp}{J_\parallel}} = 0.28, \tag{2}$$

where $t_\perp$ and $t_\parallel$ are the hopping matrix elements between nearest-neighbor copper sites perpendicular and within the CuO_2 layers, respectively. The t's are determined by quantum chemistry and are unlikely to vary significantly upon changing the oxygen content x in $YBa_2Cu_3O_{6+x}$. The anisotropy given by Eq. (2) is therefore one of the fundamental parameters characterizing the electronic state of the $YBa_2Cu_3O_{6+x}$ system. It is presumably no accident that the superconducting transition temperature, T_c, of the copper oxide superconductors tends to increase substantially as the number of consecutive CuO_2 layers increases: Electron transfer processes between directly adjacent layers (the microscopic nature of which is still controversial) are probably responsible for enhancing T_c with respect to typical single-layer materials. In some models interlayer electron transfer is even the driving force of the superconducting transition [15]. The energy scale for these processes, set by Eq. (2) and directly determined by our neutron scattering measurements, is thus an important part of a microscopic description of these materials.

3. Magnetic resonance peak in the superconducting state of $YBa_2Cu_3O_7$

We will now discuss the spin excitation spectrum of superconducting $YBa_2Cu_3O_7$ which is very different from the one of the antiferromagnetic $YBa_2Cu_3O_{6.2}$, and then show in the next section how the spectrum evolves from one extreme to the other. $YBa_2Cu_3O_7$ has 39 different phonon branches, and painstaking work is necessary to separate the cross sections of optical phonons and spin excitations. Over the years, several groups have developed an arsenal of techniques to deal with this problem; these include comparison of spectra taken in the same crystal in different oxygenation states [3], detailed monitoring of the temperature dependence of the neutron cross section [2, 3], phonon structure factor calculations [6], and spin polarization analysis [5, 6]. Together, these techniques have resulted in a detailed, reliable picture of the spin excitations of $YBa_2Cu_3O_7$, and any remaining controversies appear to have been resolved. The picture that has emerged is as elegantly simple as it is surprising.

Rossat-Mignod and coworkers [4] had first discovered a peculiar enhancement of the magnetic cross section of this compound around 40 meV at low temperatures, but the temperature dependence of this excitation was not determined. Further work on this mode was reported by Mook et al. [5]. Our recent experiments [6, 7] have revealed the following remarkable features of the 40 meV magnetic mode: First, the excitation exists only at a single point in an $(\omega, \boldsymbol{q})$ diagram (Fig. 2): The width is resolution limited in energy and close to resolution limited in $\boldsymbol{q}$, and there is no evidence for dispersion of the mode. Second, the intensity of the sharp peak is nonzero *only* in the superconducting state. Some raw data are shown in Fig. 3, and the temperature dependence of the spectral weight of the excitation is shown in Fig. 4. A careful calibration allows us to extract the dynamical spin susceptibility, χ'', from the data in absolute units. Third, as also shown in Fig. 4, the excitation energy remain constant (to within an experimental error of $\lesssim 5\%$) at least up to $T = 80$ K ($\sim 0.8 T_c$, where $T_c = 93.0$ K). Finally, the dynamical structure factor of the excitation as a function of $Q_\perp$ is $\sin^2(\pi Q_\perp zc)$, identical to the structure factor of acoustic spin waves in antiferromagnetic $YBa_2Cu_3O_{6+x}$.

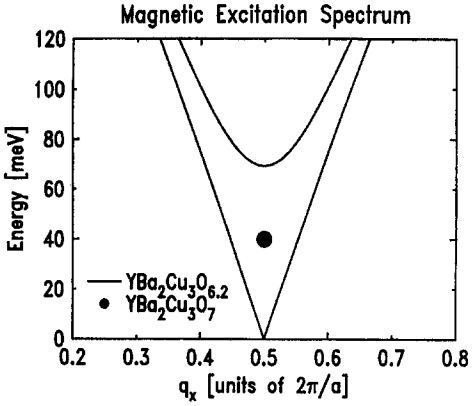

Fig. 2. (Lines) Experimentally determined dispersions of acoustic and optical spin waves in $YBa_2Cu_3O_{6.2}$. (Dot) Location of the 40 meV resonance peak in the superconducting state of $YBa_2Cu_3O_7$.

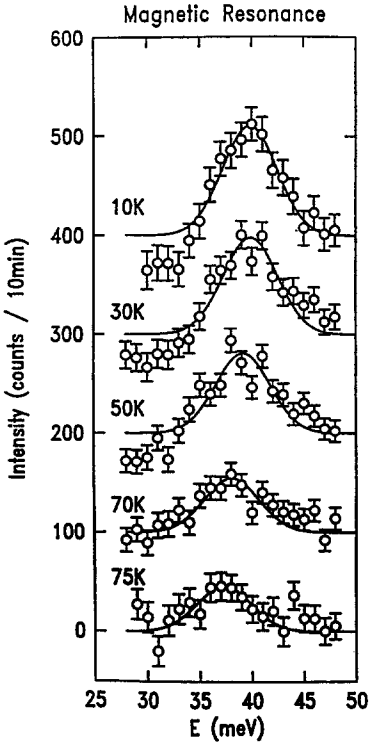

Fig. 3. Magnetic resonance peak in $YBa_2Cu_3O_7$ at $\boldsymbol{q} = (\pi, \pi)$ and at the maximum of the $\sin^2(\pi Q_\perp zc)$ dynamical structure factor as a function of energy at various temperatures. The phonon background has been subtracted (from Ref. [6]).

This magnetic resonance peak is thus a novel and unusual signature of the superconducting state in $YBa_2Cu_3O_7$. To our knowledge, similar phenomena have not been observed in any other material. Two very different explanations (with various modifications) have been proposed for our experiment, and there is as yet no consensus about its correct interpretation. However, both explanations invoke and in fact require a d-wave pairing state (or at least a gap function with sign reversal on the Fermi surface), which explains why this feature is not observed in conventional superconductors.

The first explanation [6,16–20] attributes the resonance peak to the creation of a quasielectron–quasihole pair across the superconducting energy gap. As the initial state is a singlet (Cooper pair) and the pair is created by magnetic scattering, the final state must be a triplet. The imaginary part of the dynamical susceptibility for this process is

$$\chi_0''(\boldsymbol{q},\omega) = \sum_{\boldsymbol{k}} \left(1 - \frac{\varepsilon_{\boldsymbol{k}}\varepsilon_{\boldsymbol{k}+\boldsymbol{q}} + \Delta_{\boldsymbol{k}}\Delta_{\boldsymbol{k}+\boldsymbol{q}}}{E_{\boldsymbol{k}}E_{\boldsymbol{k}+\boldsymbol{q}}}\right) \times (f_{\boldsymbol{k}+\boldsymbol{q}\uparrow} + f_{\boldsymbol{k}\downarrow} - 1)\,\delta(E_{\boldsymbol{k}+\boldsymbol{q}} + E_{\boldsymbol{k}} - \hbar\omega), \tag{3}$$

where $f_{\boldsymbol{k}}$ is the Fermi factor, $\Delta_{\boldsymbol{k}}$ is the momentum-dependent energy gap, $E_{\boldsymbol{k}} = \sqrt{\Delta_{\boldsymbol{k}}^2 + \varepsilon_{\boldsymbol{k}}^2}$ is the quasiparticle energy, and $\varepsilon_{\boldsymbol{k}}$ is the band dispersion with respect to the Fermi surface. χ_0'' is proportional to the joint density of occupied and unoccupied states and can be calculated for the band structure of $YBa_2Cu_3O_7$. The first factor is the *coherence factor* which is a consequence of the functional form of the BCS wave function. It is apparent that the coherence factor is zero on the Fermi surface ($\varepsilon_{\boldsymbol{k}} = \varepsilon_{\boldsymbol{k}+\boldsymbol{q}} = 0$) unless the gap function has opposite sign at the points $\boldsymbol{k}$ and $\boldsymbol{k}+\boldsymbol{q}$ where the two quasiparticles are created. In particular, for a d-wave gap the coherence factor is maximum for $\boldsymbol{q} \sim (\pi, \pi)$ which connects two maxima of $|\Delta_{\boldsymbol{k}}|$ with reverse sign. The energy to create a quasiparticle–quasihole pair with this relative momentum is $2\Delta_{\max}$, where $\Delta_{\max}$ is the maximum of the d-wave gap function. As we have experimentally established that the resonance peak vanishes in the normal state, we can indeed associate the resonance energy with the superconducting energy gap. The d-wave symmetry of the

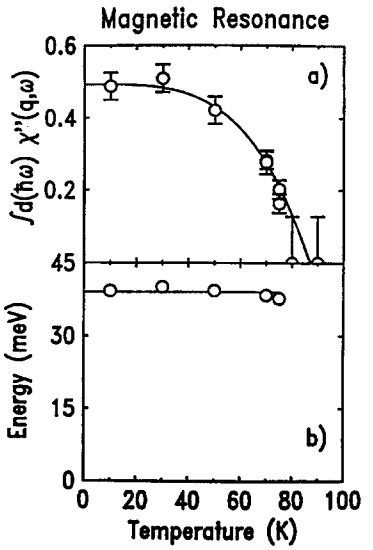

Fig. 4. (a) Absolute spectral weight and (b) maximum energy of the resonance peak as a function of temperature (from Ref. [6]).

gap function has now been firmly established by various quantum interference experiments, and our experiments confirm this result in a completely different fashion.

A detailed calculation [17] shows that $\chi_0''(\boldsymbol{q},\omega)$ evaluated at $\boldsymbol{q}=(\pi,\pi)$ as a function of $\hbar\omega$ only shows a *step* at an energy of $2\Delta_{\max}$, whereas we observe a sharp *peak*. However, the real part of the bare susceptibility, χ_0', (which is not measured in a neutron scattering experiment) *does* show a peak at this energy. Several groups [16–18] have thus invoked a renormalization of χ_0 by electron–electron interactions which can be written in the RPA approximation as

$$\chi_{\mathrm{RPA}}(\boldsymbol{q},\omega)=\frac{\chi_0(\boldsymbol{q},\omega)}{1-J(\boldsymbol{q})\chi_0(\boldsymbol{q},\omega)}. \tag{4}$$

By calculating the imaginary part of this expression one can convince oneself that the "Stoner factor" in the denominator converts the peak in χ_0' into a peak in χ_{RPA}'' if the interaction term $J(\boldsymbol{q})$ is peaked at $\boldsymbol{q}=(\pi,\pi)$. In the strongly interacting limit the quasielectron–quasihole pair may be thought of as a "triplet exciton". By tuning the functional form of $J(\boldsymbol{q})$, good agreement with the experimentally measured shape of the resonance peak can be achieved [16–18]. In an alternative scenario, nesting features of the band structure are also capable of producing a peak in χ_0'' [19]. The interlayer pair tunneling theory of Anderson and coworkers [20] can account for most features of the experiment without ad hoc adjustment of parameters. In their picture, kinematic constraints associated with the non-BCS functional form of the interlayer gap equation are responsible for the sharpness of the peak.

A very different explanation has been suggested by Zhang and collaborators [21]. Instead of a particle–hole excitation, they attribute the resonance to a *particle–particle* mode characteristic of the Hubbard model. There are actually two such modes: The one originally proposed consists of two electrons in a single state on the same site, moving with momentum $\boldsymbol{q}=(\pi,\pi)$. Creating this pair costs an energy of the order of the on-site Coulomb repulsion, but once the pair is created it has both a well-defined energy and an infinite lifetime. The first property derives from the fact that for a tight-binding band the sum of the two particle energies, $\varepsilon_{\boldsymbol{k}}+\varepsilon_{\boldsymbol{k}+\boldsymbol{q}}$, has only one possible value for $\boldsymbol{q}=(\pi,\pi)$. The pair does not decay by scattering from other electrons, because such scattering processes are forbidden by the Pauli principle. The second mode, and the one that is relevant for our experiment, is a particle–particle pair on nearest-neighbor sites in a triplet state, the creation of which costs an energy of the order of $J_{\parallel}$. These particle–particle modes exist at all temperatures, but do not couple to external probes in the normal state. In the superconducting state particle and hole states are mixed, and the cross section for creation of the triplet mode by magnetic neutron scattering is proportional to Δ^2, where Δ is the superconducting energy gap.

There are open questions about both of these different explanations. In the particle–hole picture the resonance energy should follow the temperature dependence of the superconducting energy gap, which appears hard (but perhaps not impossible) to reconcile with Fig. 4(b). For the particle–particle picture, it has not been resolved how deviations from a nearest-neighbor tight binding band structure (which seem to be necessary to account for the observed Fermi surface) affect the resonance [24]. Another open question concerns the experimentally measured dynamical structure factor of the resonance $[\sim\sin^2(\pi Q_\perp zc)]$ which has not yet been fully explained in either picture.

4. Magnetic resonance peak in underdoped $YBa_2Cu_3O_{6+x}$

In the metallic but still underoxygenated regime of the phase diagram (for $0.4 \lesssim x < 1$) antiferromagnetic long-range order vanishes but low-energy spin excitations are known to persist [2, 3]. These excitations resemble acoustic spin waves in antiferromagnetic $YBa_2Cu_3O_{6+x}$ in that their cross section is maximum around the antiferromagnetic ordering wave vector $q = (\pi, \pi)$ and they follow the dynamical structure factor which characterizes acoustic spin waves. However, in contrast to antiferromagnetic spin waves these excitations are broadened in momentum space, which implies a finite correlation length (typically only a few lattice spacings) in real space. Further, the low-energy spectral weight of these excitations is severely depressed, a phenomenon which has been termed "spin pseudo-gap" and is also observed in NMR experiments. Semiphenomenological models which include the effects of both band structure and electron–electron interactions have been developed to account for the experimental observations [25].

In order to provide more experimental input for theories of the 40 meV resonance peak, we decided to search for analogous spectral weight enhancements in the superconducting states of underdoped $YBa_2Cu_3O_{6+x}$ [8]. To this end crystals with several different oxygen concentrations were prepared. Fig. 5 shows the difference between spectra measured above and below T_c for two doping levels, $YBa_2Cu_3O_{6.5}$ ($T_c = 52$ K) and $YBa_2Cu_3O_{6.7}$ ($T_c = 67$ K). Spin polarization analysis has revealed that the observed enhancements of the magnetic cross section below the superconducting transition temperature are purely magnetic in origin. Fig. 6 shows that the additional magnetic intensity appears abruptly at the superconducting transition temperature. A similar data set has also been taken for $YBa_2Cu_3O_{6.8}$ where the enhancement is centered around 35 meV [9]. A synopsis of the presently available data is given in Fig. 7.

At least at the experimental level, a consistent picture of the effects of superconductivity on the magnetic excitation spectra of the cuprates is now beginning to emerge: Lower the transition temperature, lower the energy around which the enhancement is centered, broader the energy range over which it occurs, and smaller the fraction of the normal state

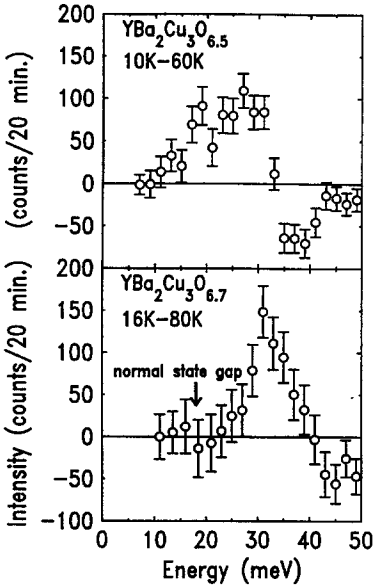

Fig. 5. Difference between the low temperature ($< T_c$) and high-temperature ($\gtrsim T_c$) magnetic intensity at $Q = (\frac{1}{2}, \frac{1}{2}, -5.4)$. The data were adjusted for the Bose factor and for a weakly temperature-dependent featureless background at low energies in the lower panel (from Ref. [8]).

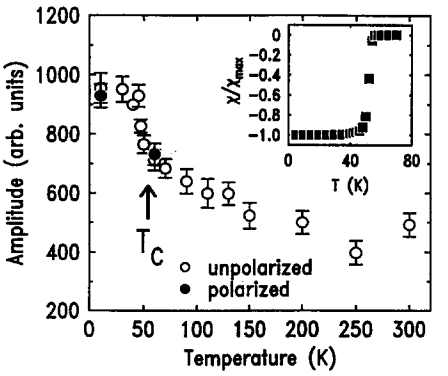

Fig. 6. The open symbols are the amplitudes of the magnetic cross section at $\hbar\omega = 25$ meV, extracted from Gaussian fits to unpolarized-beam constant-energy scans. The closed symbols are the spin-flip peak intensities measured at $Q = (\frac{3}{2}, \frac{1}{2}, -1.7)$ with a polarized beam, corrected for the background and scaled to the unpolarized-beam data. The inset shows the field-cooled DC susceptibility at $H = 10$ G measured by SQUID magnetometry on a small piece cut from the inside (not the surface) of the sample. Because of demagnetization effects the Meissner fraction was nominally > 100%. The data were therefore normalized to the maximum susceptibility (from Ref. [8]).

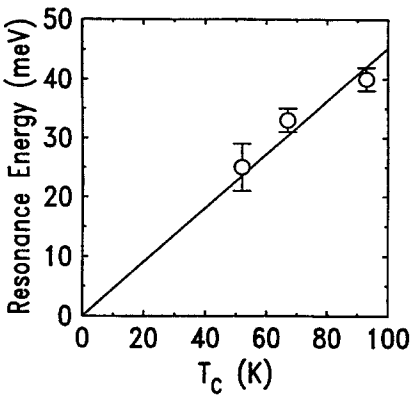

Fig. 7. Energy of maximum superconductivity-induced spectral enhancement as a function of the transition temperature T_c. For $YBa_2Cu_3O_{6.7}$ and $YBa_2Cu_3O_7$ the enhancement is resolution-limited in energy, and the error bars are upper bounds on the intrinsic width of the resonance (from Ref. [8]).

spectrum that is affected. This trend is followed also in $La_{1.86}Sr_{0.14}CuO_4$ where a very small enhancement below $T_c \sim 35$ K has recently been observed over a rather wide energy range around 10–15 meV [26]. By comparison of our recent data for $YBa_2Cu_3O_{6.5}$ with previous work in the same range of concentration in the normal state, it is also clear that, while the enhancement occurs sharply at T_c, it follows a trend already established in the normal state. This observation is presumably intimately related to recent photoemission work in underdoped cuprates which indicates that a gap-like structure in the single-particle density of states is already apparent at temperature far above T_c [27–29].

5. Phonon line shapes

Another, more indirect probe of the electronic state of $YBa_2Cu_3O_7$ is the investigation of phonon energies and lifetimes, especially their renormalization below the superconducting transition temperature. Electron–phonon scattering contributes to the finite lifetimes of phonons in the normal state, and depending on the magnitude of this contribution the lifetime of specific phonons can be affected by the redistribution of the electronic density of states in the superconducting state. This effect had been demonstrated by neutron scattering in conventional superconductors, and by Raman scattering at $\boldsymbol{q} = 0$ in high-temperature superconductors including $YBa_2Cu_3O_7$ [30, 31].

It has recently become possible to achieve high enough energy resolution in neutron scattering experiments to measure intrinsic phonon lifetimes at nonzero $\boldsymbol{q}$. We [12] have focused on an oxygen vibration of B_{1g} symmetry at 42.5 meV which had been shown by Raman scattering to exhibit the largest superconductivity-induced line shape anomalies at $\boldsymbol{q} = 0$. Harashina et al. [32] have also studied another oxygen vibration. In the normal state, the dispersion of the 42.5 meV phonon is completely flat, and the intrinsic line width (~ 2 meV) is $\boldsymbol{q}$-independent to within our resolution. In the superconducting state, Raman work has shown that at $\boldsymbol{q} = 0$ the phonon softens by almost 1 meV, and the line width broadens substantially. This can be understood on a qualitative level if 42.5 meV happens to just exceed $2\Delta_{max}$: In order to compensate for the loss of electronic states below the superconducting energy gap, there is a pileup in the density of states above the gap which in turn decreases the phonon lifetime via the electron–phonon interaction.

In a pioneering study Pyka et al. [33] had been able to measure the effect of superconductivity on the dispersion this phonon mode at nonzero $\boldsymbol{q}$. Our recent experiments [11] had sufficient resolution to also determine the lifetime of this phonon branch above and below T_c. The lifetime is quite anisotropic (Fig. 8) and is in fact much shorter at low temperatures along the (1 0 0) crystallographic direction than along (1 1 0). One factor which is certainly relevant in explaining this anisotropy is another coherence factor, analogous to the coherence factor entering Eq. (3). However, there is a crucial difference between the coherence factor entering the cross section for magnetic neutron scattering and the one entering the phonon self-energy: While magnetic neutron scattering is antisymmetric under time reversal symmetry, electron–phonon scattering is time-reversal symmetric, and the coherence factor therefore has the opposite sign [34, 35]:

$$1 + \frac{\varepsilon_k \varepsilon_{k+q} + \Delta_k \Delta_{k+q}}{E_k E_{k+q}}. \tag{5}$$

This factor is maximum for $\boldsymbol{q}$-vectors connecting two lobes of the gap function which have the same sign, that is, $\boldsymbol{q}$-vectors along (1 0 0). The experimentally

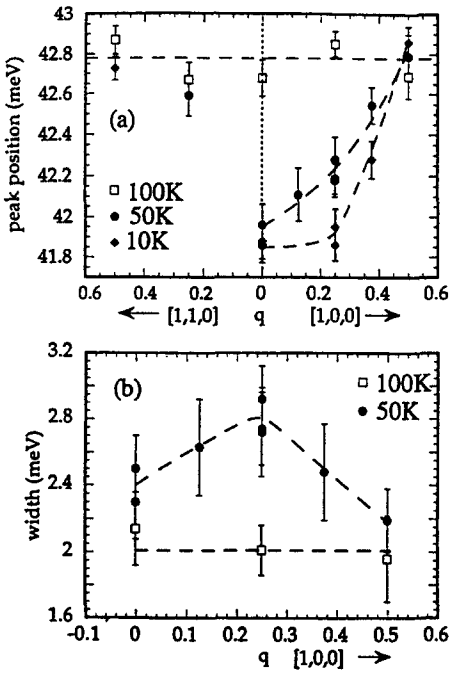

Fig. 8. a) Dispersion and b) linewidth of the 42.5 meV oxygen vibration as a function of q above and below T_c (From Ref. [12]).

observed maximum in the phonon line width (corresponding to a minimum in its lifetime) is consistent with the fact that it is at the q-vector connecting the two gap maxima along this direction [11]. A full explanation of our data will require a model of the electron–phonon interaction as well as an evaluation of the joint density of occupied and unoccupied states for the band structure of $YBa_2Cu_3O_7$. One might hope to gain further insight into the nature of the electronic state as well as the electron–phonon interaction by comparing the microscopic parameters necessary to explain our data on the magnetic resonance peak and our data on the phonon lifetime renormalization.

Acknowledgements

We thank B. Roessli, J. Kulda and P. Palleau for assistance with the measurements at the ILL, M. Braden and B. Hennion for assistance with measurements at LLB, and P.W. Anderson for helpful discussions. The work at Princeton University was supported by the MRSEC Program of the National Science Foundation under grant No. DMR-9400362, and by the Packard and Sloan Foundations. We also acknowledge the European "Human Capital and Mobility" program No. ERBCHRXCT930113 for financial support.

References

[1] J.M. Tranquada, G. Shirane, B. Keimer, M. Sato and S. Shamoto, Phys. Rev. B 40 (1989) 4503; S. Shamoto, M. Sato, J.M. Tranquada, B.J. Sternlieb and G. Shirane, ibid. 48 (1993) 13 817.
[2] J.M. Tranquada, P.M. Gehring, G. Shirane, S. Shamoto and M. Sato, Phys. Rev. B 46 (1992) 556.
[3] J. Rossat-Mignod, L.P. Regnault, P. Bourges, P. Burlet, C. Vettier and J.Y. Henry, in: Selected Topics in Superconductivity (World Scientific, Singapore, 1993); P. Bourges et al., Phys. Rev. B 53 (1996) 876.
[4] J. Rossat-Mignod, L.P. Regnault, C. Vettier, P. Bourges, P. Burlet, J. Bossy, J.Y. Henry and G. Lapertot, Physica C 185–189 (1991) 86.
[5] H.A. Mook, M. Yethiraj, G. Aeppli, T.E. Mason and T. Armstrong, Phys. Rev. Lett. 70 (1993) 3490.
[6] H.F. Fong, B. Keimer, P.W. Anderson, D. Reznik, F. Dogan and I.A. Aksay, Phys. Rev. Lett. 75 (1995) 316; B. Keimer, H.F. Fong, D. Reznik, F. Dogan and I.A. Aksay, J. Phys. Chem. Solids 56 (1995) 1927; H.F. Fong, B. Keimer, D. Reznik, D.L. Milius and I.A. Aksay, Phys. Rev. B 54 (1996) 6708.
[7] P. Bourges, L.P. Regnault, Y. Sidis and C. Vettier, Phys. Rev. B 53 (1996) 876.
[8] H.F. Fong, B. Keimer, D.L. Milius and I.A. Aksay, Phys. Rev. Lett. 78 (1997) 713.
[9] P. Bourges, L.P. Regnault, P. Burlet et al., Physics B 215 (1995) 30.
[10] D. Reznik, P. Bourges, H.F. Fong, L.P. Regnault, J. Bossy, C. Vettier, D.L. Milius, I.A. Aksay and B. Keimer, Phys. Rev. B 53 (1996) R14741.
[11] P. Bourges, H.F. Fong et al., Phys. Rev. B 54 (1996) R 6905.
[12] D. Reznik, B. Keimer, F. Dogan and I.A. Aksay, Phys. Rev. Lett. 75 (1995) 2396.
[13] O.K. Andersen et al., J. Phys. Chem. Solids 56 (1995) 1573.
[14] S.M. Hayden et al., unpublished.
[15] S. Chakravarty, A. Sudbo, P.W. Anderson and S. Strong, Science 261 (1993) 337.
[16] D.Z. Liu, Y. Zha and K. Levin, Phys. Rev. Lett. 75 (1995) 4130.
[17] I.I. Mazin and V.M. Yakovenko, Phys. Rev. Lett. 75 (1995) 4134.
[18] F. Onufrieva, Physica C 251 (1995) 348.
[19] N. Bulut and D.J. Scalapino, Phys. Rev. B 53 (1996) 5149.
[20] L. Yin, S. Chakravarty and P.W. Anderson, Report No. cond-mat/9606139; P.W. Anderson, unpublished.
[21] E. Demler and S.C. Zhang, Phys. Rev. Lett. 75 (1995) 4126.

[22] A.J. Millis and H. Monien, Phys. Rev. B 54 (1996) 16172.
[23] N. Bulut and D.J. Scalapino, Phys. Rev. B 53 (1996) 5149.
[24] H. Kohno, B. Normand and H. Fukuyama, preprint.
[25] See, e.g., Q. Si, K. Levin and J.P. Lu, Phys. Rev. B 47 (1995) 9055.
[26] T.E. Mason, G. Aeppli, S.M. Hayden and H.A. Mook, Phys. Rev. Lett. 77 (1996) 1604.
[27] D.S. Marshall, D.S. Dessau, A.G. Loeser, C.H. Park, A.Y. Matsuura, J.N. Eckstein, I. Bosovic, P. Fournier, A. Kapitulnik, W.E. Spicer and Z.X. Shen, Phys. Rev. Lett. 76 (1996) 4841.
[28] A.G. Loeser, Z.X. Shen, D.S. Dessau, D.S. Marshall, C.H. Park, P. Fournier and A. Kapitulnik, Science 273 (1996) 325.
[29] H. Ding, T. Yokoya, J.C. Campuzano, T. Takahashi, M. Randeria, M.R. Norman, T. Mochiku, K. Kadowaki and J. Giapintzakis, Nature 382 (1996) 51.
[30] M. Cardona, Physica 185–189C (1991) 65; J. Humlicek et al., Physica C 206 (1993) 345.
[31] E. Altendorf, et al. Phys. Rev. B 47 (1993) 8140.
[32] H. Harashina, K. Kodama, S. Shamoto, M. Sato, K. Kakurai and M. Nishi, J. Phys. Soc. Japan 64 (1995) 1462.
[33] N. Pyka, W. Reichardt, L. Pintschovius, G. Engel, J. Rossat-Mignod and J.Y. Henry, Phys. Rev. Lett. 70 (1993) 1457.
[34] M.E. Flatté, Phys. Rev. Lett. 70 (1993) 658.
[35] M.E. Flatté, S. Quinlan and D.J. Scalapino, Phys. Rev. B 48 (1993) 10626.